Interfaces between a fibre and its matrix

Lilholt, Hans; Sørensen, Bent F.

Published in:
I O P Conference Series: Materials Science and Engineering

Link to article, DOI:
10.1088/1757-899X/219/1/012030

Publication date:
2017

Document Version
Publisher's PDF, also known as Version of record

Interfaces between a fibre and its matrix

2017 IOP Conf. Ser.: Mater. Sci. Eng. 219 012030

(http://iopscience.iop.org/1757-899X/219/1/012030)

Interfaces between a fibre and its matrix

H Lilholt and B F Sørensen

Section of Composites and Materials Mechanics, Department of Wind Energy, Technical University of Denmark, Risø Campus, Roskilde, Denmark

E-mail: hali@dtu.dk

Abstract. The interface between a fibre and its matrix represents an important element in the characterization and exploitation of composite materials. Both theoretical models and analyses of experimental data have been presented in the literature since modern composite were developed and many experiments have been performed. A large volume of results for a wide range of composite systems exists, but rather little comparison and potential consistency have been reached for fibres and/or for matrices. Recently a materials mechanics approach has been presented to describe the interface by three parameters, the interfacial energy [J/m2], the interfacial frictional shear stress [MPa] and the mismatch strain [-] between fibre and matrix. The model has been used for the different modes of fibre pull-out and fibre fragmentation. In this paper it is demonstrated that the governing equations for the experimental parameters (applied load, debond length and relative fibre/matrix displacement) are rather similar for these test modes. A simplified analysis allows the direct determination of the three interface parameters from two plots for the experimental data. The complete analysis is demonstrated for steel fibres in polyester matrix. The analysis of existing experimental literature data is demonstrated for steel fibres in epoxy matrix and for tungsten wires in copper matrix. These latter incomplete analyses show that some results can be obtained even if all three experimental parameters are not recorded.

1. Introduction

In fibrous composite materials the fibres and matrix interact to produce the resulting properties of the composites. This interaction takes several forms. The fibres and matrix separately contribute with their "own" properties (often in a fraction-weighted way), and these properties of the constituents are both the stiffness, the stress and the strain (elongation). The fibres and the matrix also interact with each other through the interface between them and contribute additional behavior and properties. Normally composite materials are composed of (one type of) fibres of cylindrical geometry with one long dimension and two small transverse dimensions, which normally form a roughly equiaxed cross section, that is often represented by a circular cross section. The representative model for the composite is thus a straight circular fibre in a block of matrix. The interface parameters are the

interfacial energy G_{iic} [J/m^2], which is assumed to represent the chemical nature and bonding of the fibre surface to the matrix, the frictional *interfacial shear stress* τ_s [MPa], which is assumed to represent the topography and frictional sliding of the fibre relative to the matrix, and the *mismatch strain* Δe^T [-], which is caused by the thermo-elastic difference between fibre and matrix.

The first analysis of the interface was suggested by Kelly and Tyson [1], who for the system of metal wires (tungsten) in a metal matrix (copper) introduced and used the concept of a constant maximum interfacial shear stress, representing the sliding of the interface or the yielding of the near-by matrix. This concept was in the following years used in several (simple) models and related experiments, (see e.g. conference reports [2] [3]), and applied to many other combinations of fibres (e.g. glass, carbon, aramid) and matrices (e.g. polyester, epoxy, and other polymers). The one experimental method is typically the pull-out of a single fibre from a block of matrix, where the load on the fibre and the displacement of the fibre relative to the matrix are recorded. A plot of fibre load versus displacement typically shows a steeply rising initial part to a maximum load, followed by a load drop and a slowly decreasing load towards the final pulling out of the fibre from the matrix block. The maximum shear stress at the interface is typically calculated as the maximum fibre load divided by the interfacial area (equal to fibre circumference times embedded fibre length). The other experimental method is the single fibre fragmentation test, where a (mini)composite with one (brittle) fibre is loaded in tension along the fibre direction; the very low fibre volume fraction will cause multiple fracture of the fibre into a number of (short) segments, ideally of lengths between the critical fibre length and one half of the critical fibre length. This situation is the result of the concept of a constant interfacial shear stress [1], and can be used to derive the shear stress from the segment lengths and knowledge of the fibre fracture stress.

Recently, a micromechanical model including all three interface parameters has been proposed, and it has been applied to two cases of pull-out tests [4] [5] and to single fibre fragmentation test [6].

2. Micromechanical model for pull-out and single fibre fragmentation

The details of the model, its assumptions, its principles and the derivation of relevant equations have been given in the above references, and shall not be repeated here. The model includes the interface energy G_{iic}, the interface shear stress τ_s, and the mismatch strain for fibre / matrix Δe^T, as the characteristics of the interface in (fibrous) composites. The related experiments aim to record the load P_f on the fibre (pull-out cases) or the load (stress σ_c) of the composite (single fibre fragmentation case), the debond length l_d along the interface, and the relative displacement δ between fibre and matrix.

The concepts implied in the model are the *force balance* for the fibre and matrix, both at the debonding zone and far away from the zone, and including residual stresses, the *potential energy change* [7] during debonding, and the relative displacement between fibre and matrix obtained by *integration of the strain difference* along the debonded length at the interface.

The three test cases are the pull-out test with the matrix end clamped, called PO-1, the pull-out test with support of the matrix at the fibre end, called PO-2, and the single fibre fragmentation test, called SFFT. The comparative schematics for the three cases are shown in figure 1 of [5].

The model, as it has been developed [4] [5] [6], gives equations for the relations between the *experimental parameters*, the load (on fibre or on composite), the debond length, and the relative displacement. The equations include the three *interface parameters*, interface energy, interfacial shear

stress and the mismatch strain. The equations also include *materials parameters* for the fibre and the matrix, as well as the geometry of the test specimens. The parameters are listed:

Interface parameters	$Giic$	interface energy, J/m^2
	τ_s	frictional shear stress between fibre and matrix, MPa
	Δe^T	thermo-elastic mismatch strain between fibre and matrix, [-]
Material parameters	E_f	fibre stiffness, GPa
	r	fibre radius, mm
	α_f	fibre thermal expansion coefficient, K^{-1}
	E_m	matrix stiffness, GPa
	α_m	matrix thermal expansion coefficient, K^{-1}
Experimental parameters	P_f	load on the fibre, N
	σ_c	stress on the composite, MPa
	l_d	debond length along the interface, mm
	δ	relative displacement between fibre and matrix, mm
	A_c	cross sectional area of matrix block / composite, mm^2
	ΔT	test temperature minus manufacturing temperature, ^{o}C

In the original development of the model the equations were typically derived and presented as relations for the debond length as a function of relevant parameters, and for the relative displacement as a function of relevant parameters. In order to demonstrate the similarity for the three test cases, pull-out case PO-1 and PO-2, and the single fibre fragmentation case SFFT, the equations will be rewritten, to present (i) load (fibre load or composite stress) as a function of debond length and (ii) displacement/debond length ratio as a function of debond length. The first relation will give the interfacial shear stress, and the second relation will give the interfacial shear stress and the interface energy, and in combination the two relations will give the mismatch strain.

This rewriting of the original equations, the related graphical plots and the analysis of these plots will be illustrated in the following for the three test cases.

3. Common concepts and relations

Some of the concepts and related equations are identical for all three test cases, and will presented here, even if they originally were derived in slightly different form in the individual papers. These concepts are the general *force balance* and *equality of strains* at any cross section of the composite (because the composite has unidirectional and long fibres), and the *thermal stresses and strains*, as well as the *fibre stresses* and the *matrix stresses* in the uncracked composite (ahead of the debond crack tip) and in the debond region, and the *fibre strain* and the *matrix strain* in the debond region.

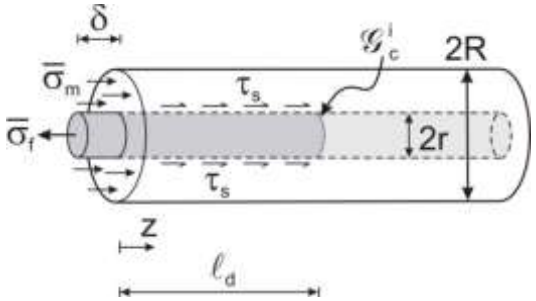

Figure 1. Geometry and loading with relevant parameters (case PO-2)

The *force balance* for the fibre and the matrix is, with sign convention as shown in figure 1:

$$P_c + (-P_f) + (-P_m) = 0$$

$$\sigma_c - V_f \cdot \sigma_f - V_m \cdot \sigma_m = 0$$

where σ is stress and V is volume fraction, with indices c for composite, f for fibre and m for matrix.

The three test cases are compared in figure 4 of [5], and the condition valid for each case is as follows:

PO-1: condition $\sigma_m = 0$, and thus $\sigma_c - V_f \cdot \sigma_f = 0$

PO-2: condition $\sigma_c = 0$, and thus $V_f \cdot \sigma_f + V_m \cdot \sigma_m = 0$

SFFT: condition $\sigma_f = 0$, and thus $\sigma_c - V_m \cdot \sigma_m = 0$

The *equality of strains* for fibre, matrix and composite implies that $e_f = e_m = e_c$.

The *thermo-elastic strains and stresses* are caused by the different stiffness (E) and thermal expansion coefficient (α) of the fibres and the matrix , respectively, and by the fact that the composite (test specimen) is manufactured at (typically) a higher temperature than the test temperature. The thermal strains (which are stress-free) of each component are

$$e_f^T = \alpha_f \cdot \Delta T \qquad \text{and} \qquad e_m^T = \alpha_m \cdot \Delta T$$

The fact that α_f and α_m (normally) are different, and assuming perfect contact at the fibre / matrix interface, means that the resulting strain for the composite is ${e_c}^T$, different from both ${e_f}^T$ and ${e_m}^T$. This leads to residual stresses in fibre and matrix:

$${\sigma_f}^{res} = E_f \cdot \left({e_c}^T - {e_f}^T \right) \qquad \text{and} \qquad {\sigma_m}^{res} = E_m \cdot \left({e_c}^T - {e_m}^T \right)$$

For the unloaded composite, these stresses are in balance by the volume fraction weighted relation:

$$V_f \cdot {\sigma_f}^{res} + V_m \cdot {\sigma_m}^{res} = 0$$

Inserting the stress expressions and solving for ${e_c}^T$, this expression for ${e_c}^T$ is re-inserted into the stress relations:

$${\sigma_f}^{res} = E_f \cdot \left(-\Delta e^T \right) \cdot \frac{V_m E_m}{E_c}$$

$${\sigma_m}^{res} = E_m \cdot \left(\Delta e^T \right) \cdot \frac{V_f E_f}{E_c}$$

$$\Delta e^T = {e_f}^T - {e_m}^T = \left(\alpha_f - \alpha_m \right) \cdot \Delta T$$

This parameter Δe^T is called the mismatch strain. It is assumed to be unknown and can be derived from the model and its equations.

The *stresses in the composite* are analyzed for two regions, the region ahead of the interface crack tip (the uncracked composite) called the up-stream region, and in the region behind the crack tip (the debond region) called the down-stream region. For the up-stream region the total stress on fibre or matrix is the sum of residual stress and mechanical stress:

$$\sigma^+ = \sigma^{res} + \sigma^{mech}$$

where the test case condition and the related stress balance (see above) as well as the equality of strains is used to derive σ^{mech}. The details for each test case are presented below. For the down-stream region the total stress σ^- on fibre or matrix is a function of the position z (figure 1) and is found from

the balance of forces, accounting for the stress transfer between fibre and matrix via the constant interfacial shear stress τ_s. For the fibre the force balance is applied at the fibre surface, for the matrix the force balance is applied at the inner surface of the matrix hole in which the fibre sits. The down-stream stresses depend on *z*-position and fulfil the force balance at any *z*-position. For the down-stream region we further need the strains for fibre and for matrix, these strains are found from the relation:

$$e^{-}(z) = e^{mech}(z) + e^{T} = \frac{\sigma^{-}(z)}{E} + e^{T}$$

where the (stress-free) thermal strain (for fibre or matrix) e^T must be added to the mechanical strain. The details for each test case are presented below.

A relation between the load (on fibre or on composite) and the debond length is established via the concept of *potential energy change* [7] during debonding. This requires the up-stream stresses for fibre and matrix and the down-stream stresses for fibre and matrix in the form:

$\sigma_f^+ - \sigma_f^-(z)$ and $\sigma_m^+ - \sigma_m^-(z)$

The derivations are explained in detail in the original papers [4] [5] [6].

A relation between the load (on fibre or on composite), the debond length and the relative displacement between fibre and matrix in the debond region (down-stream) is established by *integration of the strain difference* along the debonded length at the interface from $z = 0$ to $z = l_d$. This requires the down-stream strains for fibre and matrix in the form:

$e_f^-(z) - e_m^-(z)$

The derivations are explained in detail in the original papers [4] [5] [6].

4. Pull-out case PO-1

This pull-out case represents the most often used test geometry. The model was presented [4] [8] with a detailed analysis and comments to the assumptions and concepts used to obtain the model. Here the results are presented and rewritten into a form, which is comparable to the other test cases. The load condition is $\sigma_m = 0$, and the force balance is thus $\sigma_c - V_f \cdot \sigma_f = 0$.

The up-stream stresses are

$$\sigma_f^+ = E_f \cdot \left(-\Delta e^T\right) \cdot \frac{V_m E_m}{E_c} + E_f \cdot \frac{\sigma_c}{E_c}$$

$$\sigma_m^+ = E_m \cdot \left(+\Delta e^T\right) \cdot \frac{V_f Ef}{E_c} + E_m \cdot \frac{\sigma_c}{E_c}$$

The down-stream stresses are

$$\sigma_f^-(z) = \sigma_f - 2 \cdot \frac{\tau_s}{r} \cdot z$$

$$\sigma_m^-(z) = \frac{V_f}{V_m} \cdot 2 \cdot \frac{\tau_s}{r} \cdot z$$

The down-stream strains are

$$e_f^-(z) = \frac{\sigma_f}{E_f} - 2 \cdot \frac{\tau_s}{E_f \cdot r} \cdot z + e_f^T$$

$$e_m^-(z) = \frac{V_f E_f}{V_m E_m} \cdot 2 \cdot \frac{\tau_s}{E_f \cdot r} \cdot z + e_m^T$$

The relation between stress (load) on the fibre σ_f and debond length l_d is [4] [8]:

$$\frac{l_d}{r} = \left(\frac{E_f}{2\tau_s}\right) \cdot \left(\frac{V_m E_m}{E_c}\right) \cdot \left(\frac{\sigma_f}{E_f} + \Delta e^T\right) - \frac{E_f}{\tau_s} \cdot \sqrt{\frac{V_m E_m}{E_c} \cdot \frac{G_{iic}}{E_f \cdot r}} \quad (1)$$

The load on the fibre P_f $(= \sigma_f \cdot \pi r^2)$ is written as a function of l_d:

$$P_f = \left[2 \cdot \pi r^2 \cdot E_f \cdot \sqrt{\frac{E_c}{V_m E_m} \cdot \frac{G_{iic}}{E_f \cdot r}} - \pi r^2 \cdot E_f \cdot \Delta e^T\right] + \left[\frac{E_c}{V_m E_m} \cdot 2 \cdot \pi r \cdot \tau_s\right] \cdot l_d \quad (2)$$

This indicates a linear plot of P_f *vs* l_d, with slope and cut-off on y-axis given as

$$\text{slope} = \text{SL1} = \left[\frac{E_c}{V_m E_m} \cdot 2 \cdot \pi r \cdot \tau_s\right]$$

$$\text{cut-off} = \text{CO1} = \left[2 \cdot \pi r^2 \cdot E_f \cdot \sqrt{\frac{E_c}{V_m E_m} \cdot \frac{G_{iic}}{E_f \cdot r}} - \pi r^2 \cdot E_f \cdot \Delta e^T\right]$$

The relation between stress (load) on the fibre σ_f, the debond length l_d, and and the relative displacement between fibre and matrix δ is [4] [8]:

$$\frac{\delta}{r} = \left(\frac{\sigma_f}{E_f} + \Delta e^T\right) \cdot \frac{l_d}{r} - \frac{\tau_s}{E_f} \cdot \frac{E_c}{V_m E_m} \cdot \left(\frac{l_d}{r}\right)^2$$

The ratio δ/l_d is rewritten as a function of l_d, using the term $(\sigma_f/E_f + \Delta e^T)$ from eq (1):

$$\frac{\delta}{l_d} = \left[2 \cdot \sqrt{\frac{E_c}{V_m E_m} \cdot \frac{G_{iic}}{E_f \cdot r}}\right] + \left[\frac{E_c}{V_m E_m} \cdot \frac{\tau_s}{E_f \cdot r}\right] \cdot l_d \quad (3)$$

This indicates a linear plot of δ/l_d *vs* l_d, with slope and cut-off on y-axis given as

$$\text{slope} = \text{SL2} = \left[\frac{E_c}{V_m E_m} \cdot \frac{\tau_s}{E_f \cdot r}\right]$$

$$\text{cut-off} = CO2 = \left[2 \cdot \sqrt{\frac{E_c}{V_m E_m} \cdot \frac{G_{iic}}{E_{f \cdot r}}} \right]$$

The two (linear) equations (2) and (3) allow the three interface parameters to be determined from two linear plots. Eq (2) gives the interface shear stress τ_s from the slope SL1, and yields a *combination* of G_{iic} and Δe^T from the cut-off CO1. Eq (3) gives the interface shear stress τ_s from the slope SL2, and the interface energy G_{iic} from the cut-off CO2. Inserting this value for G_{iic} into CO1 gives a value for Δe^T:

$$\Delta e^T = CO2 - \frac{CO1}{\pi r^2 \cdot E_f}$$

5. Pull-out case PO-2

This pull-out case has been used in some tests and implies a clamping device to support the matrix block at the fibre end of the specimen. The practical geometry has often been a drop of matrix (polymer) on the fibre, which is pulled out of this drop. The macroscopic specimen geometry of this droplet test is not well defined. The present model (which implies a circular cylindrical geometry) was presented [5] with a detailed analysis and comments to the assumptions and concepts used to obtain the model. Here the results are presented and rewritten into a form, which is comparable to the other test cases. The load condition is $\sigma_c = 0$, and the force balance is thus $V_f \cdot \sigma_f + V_m \cdot \sigma_m = 0$.
The up-stream stresses are

$$\sigma_f^+ = E_f \cdot \left(-\Delta e^T \right) \cdot \frac{V_m E_m}{E_c}$$

$$\sigma_m^+ = E_m \cdot \left(+\Delta e^T \right) \cdot \frac{V_f Ef}{E_c}$$

It should be noted that the second term with σ_c/E_c is not present because the condition is $\sigma_c = 0$.
The down-stream stresses are

$$\sigma_f^-(z) = \sigma_f - 2 \cdot \frac{\tau_s}{r} \cdot z$$

$$\sigma_m^-(z) = \frac{V_f}{V_m} \cdot \left(2 \cdot \frac{\tau_s}{r} \cdot z - \sigma_f \right)$$

The down-stream strains are

$$e_f^-(z) = \frac{\sigma_f}{E_f} - 2 \cdot \frac{\tau_s}{E_f \cdot r} \cdot z + e_f^T$$

$$e_m^-(z) = \frac{V_f E_f}{V_m E_m} \cdot \left(2 \cdot \frac{\tau_s}{E_f \cdot r} \cdot z - \frac{\sigma_f}{E_f} \right) + e_m^T$$

The relation between stress (load) on the fibre σ_f and debond length l_d is ([5] eq 18):

$$\frac{\sigma_f}{E_f} = 2 \cdot \sqrt{\frac{V_m E_m}{E_c} \cdot \frac{G_{iic}}{E_f \cdot r}} - \frac{V_m E_m}{E_c} \cdot \Delta e^T + 2 \cdot \frac{\tau_s}{E_f \cdot r} \cdot l_d \tag{4}$$

The load on the fibre P_f ($= \sigma_f \cdot \pi r^2$) is written as a function of l_d:

$$P_f = \left[2 \cdot \pi r^2 \cdot E_f \cdot \sqrt{\frac{V_m E_m}{E_c} \cdot \frac{G_{iic}}{E_f \cdot r}} - \frac{V_m E_m}{E_c} \cdot \pi r^2 \cdot E_f \cdot \Delta e^T \right] + \left[2 \cdot \pi r \cdot \tau_s \right] \cdot l_d \tag{5}$$

This indicates a linear plot of P_f *vs* l_d, with slope and cut-off on y-axis given as

$$\text{slope} = \text{SL1} = \left[2 \cdot \pi r \cdot \tau_s \right]$$

$$\text{cut-off} = \text{CO1} = \left[2 \cdot \pi r^2 \cdot E_f \cdot \sqrt{\frac{V_m E_m}{E_c} \cdot \frac{G_{iic}}{E_f \cdot r}} - \frac{V_m E_m}{E_c} \cdot \pi r^2 \cdot E_f \cdot \Delta e^T \right]$$

It should be noted that eq (5) is similar to eq (2) of case PO-1, with the scaling factor $V_m E_m / E_c$, such that loads (stresses) on the fibre relate *by* $P_f(PO\text{-}2) = V_m E_m / E_c \cdot P_f(PO\text{-}1)$.

The relation between stress (load) on the fibre σ_f, the debond length l_d, and the relative displacement between fibre and matrix δ is ([5] eq 11):

$$\frac{\delta}{r} = \left(\frac{E_c}{V_m E_m} \cdot \frac{\sigma_f}{E_f} + \Delta e^T \right) \cdot \frac{l_d}{r} - \frac{E_c}{V_m E_m} \cdot \frac{\tau_s}{E_f} \cdot \left(\frac{l_d}{r} \right)^2$$

The ratio δ / l_d is rewritten as a function of l_d, using the term $(E_c / V_m E_m \cdot \sigma_f / E_f + \Delta e^T)$ from eq (4):

$$\frac{\delta}{l_d} = \left[2 \cdot \sqrt{\frac{E_c}{V_m E_m} \cdot \frac{G_{iic}}{E_{f \cdot r}}} \right] + \left[\frac{E_c}{V_m E_m} \cdot \frac{\tau_s}{E_f \cdot r} \right] \cdot l_d \tag{6}$$

This indicates a linear plot of δ / l_d *vs* l_d, with slope and cut-off on y-axis given as

$$\text{slope} = \text{SL2} = \left[\frac{E_c}{V_m E_m} \cdot \frac{\tau_s}{E_f \cdot r} \right]$$

$$\text{cut-off} = \text{CO2} = \left[2 \cdot \sqrt{\frac{E_c}{V_m E_m} \cdot \frac{G_{iic}}{E_{f \cdot r}}} \right]$$

It should be noted that eq (6) is identical to eq (3) of case PO-1.

The two (linear) equations (5) and (6) allow the three interface parameters to be determined from two linear plots. Eq (5) gives the interface shear stress τ_s from the slope SL1, and yields a *combination* of G_{iic} and Δe^T from the cut-off CO1. Eq (6) gives the interface shear stress τ_s from the slope SL2, and

the interface energy G_{iic} from the cut-off CO2. Inserting this value for G_{iic} into CO1 gives a value for Δe^T:

$$\Delta e^T = CO2 - \frac{CO1}{\pi r^2 \cdot E_f \cdot \frac{V_m E_m}{E_c}}$$

It should be noted that although eq (3) for case PO-1 and eq (6) for PO-2, respectively, are identical, the relations to find Δe^T are not identical, but (partly) scaled by the factor $V_m E_m / E_c$.

6. Single fibre fragmentation case SFFT

This test case represents a different test geometry and specimen geometry, as well as a different progress of the experiment. In the pull-out cases, one specimen gives one set of data. In the SFFT experiment, the (single) fibre will break several times (multiple fracture), and each fibre break gives two fibre ends which retract into the hole of the matrix, giving two sets of data for load, debond length and relative fibre/matrix displacement. This event is repeated at the next fibre break, and this continues until the composite fails. The (potentially) many fibre breaks cause concern over the possible interaction of the debond lengths from nearby fibre breaks. No experiments exist to illustrate the importance of this (possible) course of events.

The model was presented [6] with a detailed analysis and comments to the assumptions and concepts used to obtain the model. Here the results are presented and rewritten into a form, which is comparable to the other test cases. The load condition is $\sigma_f = 0$, and the force balance is thus $\sigma_c - V_m \cdot \sigma_m = 0$.

The up-stream stresses are

$$\sigma_f^+ = E_f \cdot \left(-\Delta e^T\right) \cdot \frac{V_m E_m}{E_c} + E_f \cdot \frac{\sigma_c}{E_c}$$

$$\sigma_m^+ = E_m \cdot \left(+\Delta e^T\right) \cdot \frac{V_f Ef}{E_c} + E_m \cdot \frac{\sigma_c}{E_c}$$

The down-stream stresses are

$$\sigma_f^-(z) = 2 \cdot \frac{\tau_s}{r} \cdot z$$

$$\sigma_m^-(z) = \frac{\sigma_c}{V_m} - \frac{V_f}{V_m} \cdot 2 \cdot \frac{\tau_s}{r} \cdot z$$

The down-stream strains are

$$e_f^-(z) = 2 \cdot \frac{\tau_s}{E_f \cdot r} \cdot z + e_f^T$$

$$e_m^-(z) = \frac{\sigma_c}{V_m E_m} - \frac{V_f E_f}{V_m E_m} \cdot 2 \cdot \frac{\tau_s}{E_f \cdot r} \cdot z + e_m^T$$

The relation between stress on the composite σ_c and debond length l_d is ([6] eq 22):

$$\frac{\sigma_c}{E_c} = 2 \cdot \sqrt{\frac{V_m E_m}{E_c} \cdot \frac{G_{iic}}{E_f \cdot r}} + \frac{V_m E_m}{E_c} \cdot \Delta e^T + 2 \cdot \frac{\tau_s}{E_f \cdot r} \cdot l_d \tag{7}$$

The stress on the composite σ_c is written as a function of l_d:

$$\sigma_c = \left[2 \cdot E_c \cdot \sqrt{\frac{V_m E_m}{E_c} \cdot \frac{G_{iic}}{E_f \cdot r}} + V_m E_m \cdot \Delta e^T \right] + \left[E_c \cdot 2 \cdot \frac{\tau_s}{E_f \cdot r} \right] \cdot l_d \tag{8}$$

It should be noted, in contrast to the pull-out cases, that for the SFFT case (only) the composite stress (load) can be recorded experimentally, and thus eq (8) must be written in terms of σ_c .This indicates a linear plot of σ_c *vs* l_d, with slope and cut-off on y-axis given as

$$\text{slope} = \text{SL1} = \left[E_c \cdot 2 \cdot \frac{\tau_s}{E_f \cdot r} \right]$$

$$\text{cut-off} = \text{CO1} = \left[2 \cdot E_c \cdot \sqrt{\frac{V_m E_m}{E_c} \cdot \frac{G_{iic}}{E_f \cdot r}} + V_m E_m \cdot \Delta e^T \right]$$

The relation between stress on the composite σ_c , the debond length l_d, and the relative displacement between fibre and matrix δ is ([6] eq 27):

$$\frac{\delta}{r} = \left(\frac{\sigma_c}{V_m E_m} - \Delta e^T \right) \cdot \frac{l_d}{r} - \frac{E_c}{V_m E_m} \cdot \frac{\tau_s}{E_f} \cdot \left(\frac{l_d}{r} \right)^2$$

The ratio δ/l_d is rewritten as a function of l_d, using the term $(\sigma_c / V_m E_m - \Delta e^T)$ from eq (7):

$$\frac{\delta}{l_d} = \left[2 \cdot \sqrt{\frac{E_c}{V_m E_m} \cdot \frac{G_{iic}}{E_{f \cdot r}}} \right] + \left[\frac{E_c}{V_m E_m} \cdot \frac{\tau_s}{E_f \cdot r} \right] \cdot l_d \tag{9}$$

This indicates a linear plot of δ/l_d *vs* l_d, with slope and cut-off on y-axis given as

$$\text{slope} = \text{SL2} = \left[\frac{E_c}{V_m E_m} \cdot \frac{\tau_s}{E_f \cdot r} \right]$$

$$\text{cut-off} = \text{CO2} = \left[2 \cdot \sqrt{\frac{E_c}{V_m E_m} \cdot \frac{G_{iic}}{E_{f \cdot r}}} \right]$$

It should be noted that eq (9) is identical to eq (3) of case PO-1, and to eq (6) of case PO-2. The two (linear) equations (8) and (9) allow the three interface parameters to be determined from two linear plots. Eq (8) gives the interface shear stress τ_s from the slope SL1, and yields a *combination* of G_{iic}

and Δe^T from the cut-off CO1. Eq (9) gives the interface shear stress τ_s from the slope SL2, and the interface energy G_{iic} from the cut-off CO2. Inserting this value for G_{iic} into CO1 gives a value for Δe^T:

$$\Delta e^T = -CO2 + \frac{CO1}{V_m E_m}$$

It should be noted that although eq (3) for case PO-1 and eq (6) for PO-2 and eq (9) for SFFT are identical, the relations to find Δe^T are not identical, but (partly) scaled by the factor $V_m E_m$.

7. Experimental test and analysis

The three test cases have similarities and some marked differences. The two pull-out cases give one set of experimental data (fibre load P_f, debond length l_d, and relative fibre/matrix displacement δ) for each specimen. In the SFFT case, one specimen (potentially) gives several (double) sets of data. The (potentially) many fibre breaks cause concern over the possible interaction of the debond lengths from nearby fibre breaks. No experiments exist to illustrate the importance of this (possible) course of events.

There are two equations for each test case, both giving a linear plot, where the slope and the cut-off values form the basis for calculating the (three) interface parameters. The experimental data and their analysis are summarized here.

7.1 Pull-out case PO-1

The plot of P_f *vs* l_d gives the interface shear stress from the slope SL1 as

$$\tau_s = \frac{V_m E_m}{E_c} \cdot \frac{1}{2\pi r} \cdot SL1$$

The plot of δ/l_d *vs* l_d gives the interface shear stress from the slope SL2 as

$$\tau_s = \frac{V_m E_m}{E_c} \cdot E_f \cdot r \cdot SL2$$

and the interface energy G_{iic} from the cut-off CO2 as

$$G_{iic} = \frac{V_m E_m}{E_c} \cdot E_f \cdot r \cdot \frac{(CO2)^2}{4}$$

and the mismatch strain Δe^T as

$$\Delta e^T = CO2 - \frac{CO1}{\pi r^2 \cdot E_f}$$

7.2 Pull-out case PO-2

The plot of P_f *vs* l_d gives the interface shear stress from the slope SL1 as

$$\tau_s = \frac{1}{2\pi r} \cdot SL1$$

The plot of δ/l_d *vs* l_d gives the interface shear stress from the slope SL2 as

$$\tau_s = \frac{V_m E_m}{E_c} \cdot E_f \cdot r \cdot SL2$$

and the interface energy G_{iic} from the cut-off CO2 as

$$G_{iic} = \frac{V_m E_m}{E_c} \cdot E_f \cdot r \cdot \frac{(CO2)^2}{4}$$

and the mismatch strain Δe^T as

$$\Delta e^T = CO2 - \frac{CO1}{\pi r^2 \cdot E_f \cdot \frac{V_m E_m}{E_c}}$$

7.3 Single fibre fragmentation case SFFT

The plot of σ_c *vs* l_d gives the interface shear stress from the slope SL1 as

$$\tau_s = \frac{1}{2 \cdot E_c} \cdot E_f \cdot r \cdot SL1$$

The plot of δ/l_d *vs* l_d gives the interface shear stress from the slope SL2 as

$$\tau_s = \frac{V_m E_m}{E_c} \cdot E_f \cdot r \cdot SL2$$

and the interface energy G_{iic} from the cut-off CO2 as

$$G_{iic} = \frac{V_m E_m}{E_c} \cdot E_f \cdot r \cdot \frac{(CO2)^2}{4}$$

and the mismatch strain Δe^T as

$$\Delta e^T = -CO2 + \frac{CO1}{V_m E_m}$$

It should be noted that the equations governing the calculations from the experimental analyses, are rather similar and in some situations identical.

8. Discussion

8.1 Model characteristics

The model is basically one and the same, and is applied to slightly different loading cases. This leads to the rather high degree of similarity for the various equations for load vs debond length and for displacement/debond length vs debond length, and to the scaling for the pull-out cases PO-1 and PO-2 as indicated above. It should be noted that the load vs debond length equation is individual for the three test cases, while the delta/debond length vs debond length equation is identical for all three test cases and is independent of load. This is expected because the delta and the debond length are both

connected to the geometry of the debond process. This process is essentially a shear crack (mode II crack) of the interface, which is characterized by the interface energy (chemical nature) and the interfacial shear stress (interface topography).

This combined situation gives two linear equations, which are the basis for the simple and "smart" linear plots, leading to establishing the three characteristic interface parameters, as described above in the analyses.

8.2 Case $V_f = 0$

The equations have all been written with the term $V_m E_m/E_c$ as a practical term, entering the equations where required. This term is normally very close 1, because normally one rather thin fibre is embedded in a fairly large block of matrix, which makes the fibre volume fraction very low, and thus the matrix volume fraction V_m very close to 1 and E_c very close to E_m. This fact can be used to simplify the equations by setting $V_m E_m/E_c = 1$. This situation is not always present as the experimental examples below illustrates.

8.3 Traditional experiments

Many interface characterizations and related *pull-out experiments* have been reported in the literature, e.g. [9] [10] [11] for the end-gripped test geometry PO-1, and [12] [13] for the droplet test geometry PO-2. The tests have normally been performed by using several specimens with different embedded lengths of fibre. The curve for pull-out force (stress) vs fibre displacement is described in detail in [5] and figure 2. In most cases an *apparent* interfacial shear stress has been calculated from the maximum pull-out force P_{max} and the embedded fibre length l_{emb}.

$$\tau_{app} = \frac{P_{max}}{2 \cdot \pi \, r \cdot l_{emb}}$$

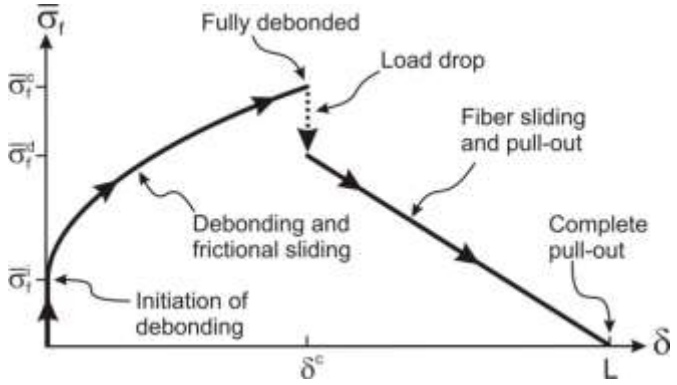

Figure 2. Sketch (not to scale) of fibre stress vs displacement between fibre and matrix for a traditional pull-out experiment with embedded fibre length L

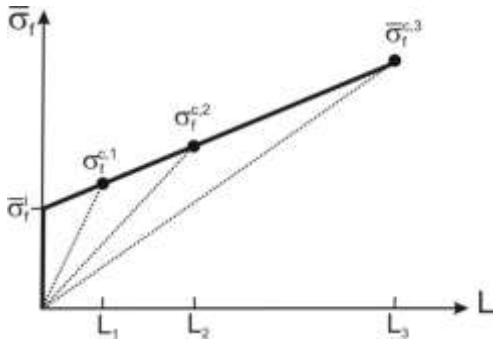

Figure 3. Sketch of the relation between fibre stress and debond length according to eq (2) and (5) for traditional pull-out experiments, the dotted slopes indicate the calculations of the *apparent* shear stress, which for this case is *decreasing* with increasing embedded fibre length (termed L)

It has often been noted in the individual publications in the literature, that this apparent shear stress was dependent on the embedded length, as discussed in [5] and illustrated in figure 3. This dependency is caused by the fact that the (maximum) fibre load is linear with but not directly proportional to embedded length. For the sake of clarity the eqs (2) and (5) for test cases PO-1 and PO-2, respectively, are written with the term $V_m E_m / E_c = 1$, making the two test cases and equations identical:

$$P_f = \left[2 \cdot \pi r^2 \cdot E_f \cdot \sqrt{\frac{G_{iic}}{E_f \cdot r}} - \pi r^2 \cdot E_f \cdot \Delta e^T \right] + \left[2 \cdot \pi r \cdot \tau_s \right] \cdot l_d \qquad (10)$$

At the maximum fibre load P_{max} the embedded fibre has debonded completely, as sketched in figure 2, and starts to pull out of the matrix block (against frictional sliding). Therefore, at $l_d = l_{emb}$ the fibre load is $P_f = P_{max}$. From this equation (10) the *apparent* shear stress can be written

$$\tau_{app} = \frac{P_{max}}{2 \cdot \pi r \cdot l_{emb}} = \frac{[constant]}{l_{emb}} + \tau_s$$

The constant is controlled by G_{iic} and Δe^T (and material parameters), and only if this constant happens to be zero, will the *apparent* shear stress give the *true* interfacial shear stress τ_s. For all other situations the apparent shear stress will depend on the embedded length, with increasing or decreasing values dependent on the sign of the constant, as discussed in [5] and figure 3. The equation (10) suggests a direct way of making a correct analysis of simple pull-out experiments, based on various embedded fibre lengths and recorded maximum force from the pull-out curve, (figure 2): by plotting the P_{max} *vs* l_{emb} and using a linear fitting equation, the slope will give the true interfacial shear stress τ_s, and the cut-off will give a constant including a combination of G_{iic} and Δe^T, but it will not allow a determination of these two parameters individually. Examples will be given below to illustrate this incomplete analysis of pull-out experiments from the literature.

9. Practical examples

The model and its method of analysis will be illustrated by three examples. The one example is a complete experiment for steel fibres in polyester matrix, where all three experimental parameters load, debond length and relative displacement are recorded. The other two examples are incomplete and are from the literature, one is steel fibres in epoxy and one is tungsten wires in copper matrix. The relevant properties for the materials systems are collected in Table 1.

Table 1. Materials properties for the practical examples

Fibre-Matrix system	Steel-Polyester	Steel-Epoxy	Tungsten-Copper
Fibre stiffness E_f, GPa	210	200	400
Fibre radius r, mm	0.155	0.075	0.25
Fibre thermal expansion, α_f, 10^{-6} K^{-1}	11.7	11.7	4.3
Matrix stiffness E_m, GPa	3	3	100
Matrix thermal expansion, α_m, 10^{-6} K^{-1}	70	50	16.5
Specimen area A_c, mm^2	25	20	28
$V_m E_m/E_c$	0.825	0.944	0.973

9.1 Steel fibres in polyester matrix (complete analysis)

The pull-out process is case PO-1 with gripping of the matrix block. These experimental data from Prabhakaran et al [8] have been analyzed earlier, using a slightly more complex procedure [8], where the specimens and the experimental test fixture is described in detail. From the video recording of the debond process a total of 30 pictures were used to measure the debond length l_d at the corresponding fibre load P_f. From the (continuous) recordings of the relative fibre/matrix displacement, (30) values for δ were selected at these fibre loads. These (30) simultaneous sets of data are the basis for establishing the plot of P_f *vs* l_d in figure 4 and the plot of δ/l_d *vs* l_d in figure 5. The experimental and material parameters are listed in Table 1. It should be noted that with the fairly thick fibre of radius 0.155 mm the fibre volume fraction of 0.003 clearly is not close to zero, and thus the parameter $V_m E_m/E_c$ is about 0.825 and must be included in the calculations. The straight lines in the plots show rather good fit (R^2 is ca. 0.98). From the slopes and cut-offs of the straight lines the three interface parameters are calculated using the equations for case PO-1 from section 7.1. The results are shown here:

SL1	1.496	N/mm
CO1	12.259	N
τ_s	1.3	MPa
SL2	0.00006164	mm^{-1}
CO2	0.002153	
τ_s	1.6	MPa
G_{iic}	31	J/m^2
Δe^T	0.0014	

It is noted that the two plots give slightly different values for the interface shear stress τ_s , it is not clear whether this is caused by experimental scatter, or whether the model and/or the analysis has a systematic deviation. The experimental mismatch strain might be compared to an estimate from its definition, this requires knowledge of the thermal expansion coefficients for fibre and matrix and also

the temperature difference between manufacturing temperature and test temperature. With reasonable assumptions as listed in Table 1, the estimated value is: $\Delta eT = (12 - 70) \cdot 10^{-6} \cdot (20 - 50) = 0.0017$.

A comparison with the results of the previous analysis [8] shows that the shear stress is very closely the same, while the interface energy and the mismatch strain deviate significantly.

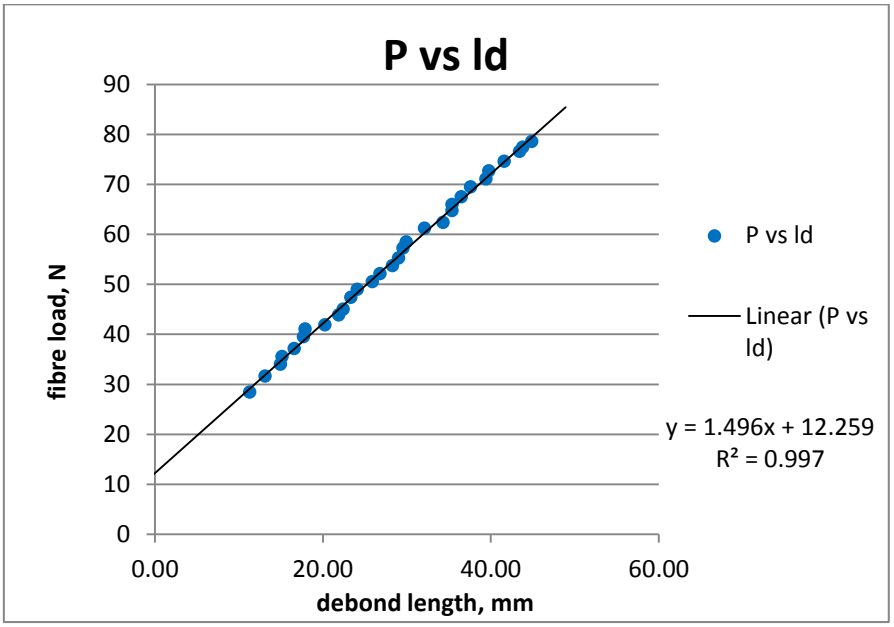

Figure 4. Experimental data for steel fibre in polyester

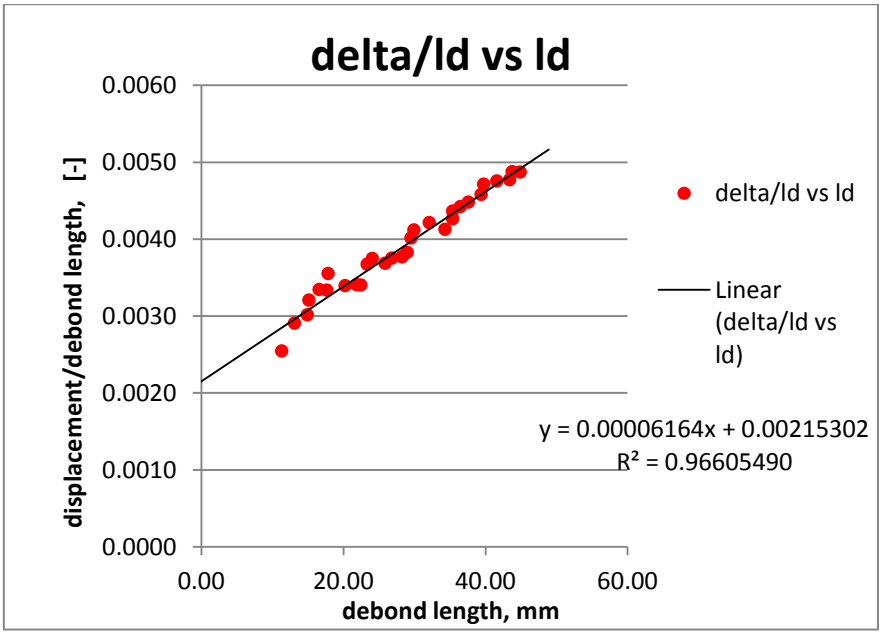

Figure 5. Experimental data for steel fibre in polyester

9.2 Steel fibres in epoxy matrix (incomplete analysis)

The pull-out process is case PO-2 with a clamp at fibre end of the specimen (droplet test). The experiments follow the traditional pull-out procedure with measurement of the maximum force for various embedded fibre lengths. The data originate from Gorbatkina [14] and were presented by Zhandarov and Mäder [15] in their figure 4b. The (7) sets of data for maximum force and embedded fibre length are analyzed according to the procedure described above for traditional, incomplete data and plotted as P_{max} *vs* l_{emb} in figure 6. The experimental and material parameters are listed in Table 1. It should be noted that with the moderately thick fibre of radius 0.075 mm the fibre volume fraction of 0.0009 clearly is not close to zero, and thus the parameter $V_m E_m/E_c$ is about 0.944 and must be included in the calculations. The straight line in figure 6 shows rather good fit (R^2 is ca. 0.94). From the slope for the straight line, the interface shear stress is calculated using the equation for P_{max} *vs* l_{emb} in the full form eq (5) for case PO-2 from section 7.2. The results are shown here:

SL1	8.847	N/mm
CO1	15.533	N
τ_s	18.8	MPa

As emphasized above the cut-off CO1 only gives a combination of G_{iic} and Δe^T. If the mismatch strain is estimated from its definition and the data in Table 1, the value is $\Delta eT = (12 - 50) \cdot 10^{-6} \cdot (20 - 120) = 0.0038$, and with this value the interface energy is ca 250 J/m^2.

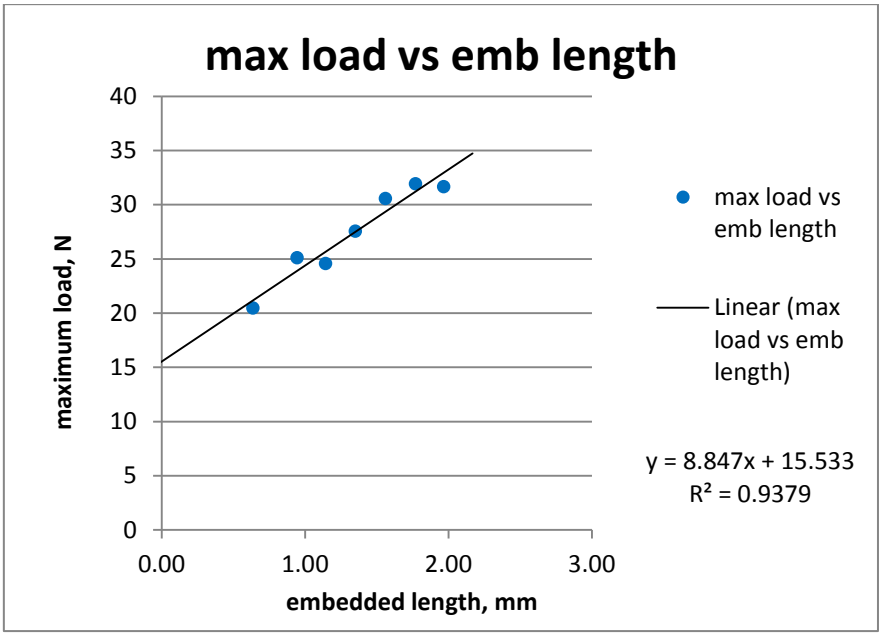

Figure 6. Experimental data for steel fibre in epoxy matrix

9.3 Tungsten wires in copper matrix (incomplete analysis)

The study of the interface in composites was (probably) initiated in the early 1960´s, and Tyson [16] performed some of the first pull-out tests for tungsten wires in blocks of copper matrix. One of these

test series, which is presented by Kelly [17] figure 5.18, is performed at 600 °C, and includes 8 sets of data for embedded fibre length and maximum force for the pull-out experiment. The test case is PO-1. The 8 sets of data are analyzed according to the procedure described above for traditional, incomplete data and plotted as P_{max} *vs* l_{emb} in figure 7. The experimental and material parameters are listed in Table 1. It should be noted that with the moderately thick fibre of radius 0.25 mm the fibre volume fraction of 0.007 clearly is not close to zero, and thus the parameter $V_m E_m/E_c$ is about 0.973 and must be included in the calculations. The straight line in figure 7 shows rather good fit (R^2 is ca. 0.94). From the slope for the straight line the interface shear stress is calculated using the equation for P_{max} *vs* l_{emb} in the full form eq (2) for case PO-1 from section 7.1. The results are shown here:

SL1	47.863	N/mm
CO1	28.326	N
τ_s	29.6	MPa

As emphasized above the cut-off CO1 only gives a combination of G_{iic} and Δe^T. If the mismatch strain is estimated from its definition and the data in Table 1, the value is $\Delta eT = (4.3 - 16.5) \cdot 10^{-6} \cdot (600 - 800) = 0.0024$, and with this value the interface energy is ca 190 J/m^2. It must be emphasized that this rough calculation is based on an effective manufacturing and stress-free state for the copper matrix at about 800 °C.

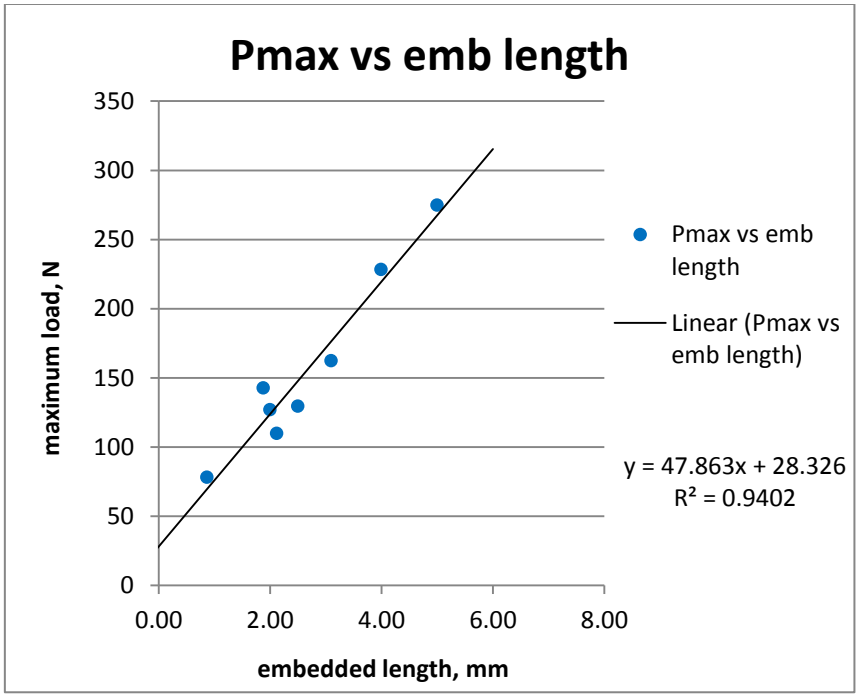

Figure 7. Experimental data for tungsten wire in copper matrix

10. Summary

The *characterization of the interface* between fibre and matrix in composites has been discussed and three interface parameters have been defined: the interface energy G_{iic} , the frictional interfacial shear stress τ_s and mismatch strain between fibre and matrix Δe^T.

The (new) *mechanical model* for the interface has been presented, and it has been based on the (three) test cases: pull-out of a fibre from a block of matrix, (i) supported by gripping at the matrix end of the specimen, called case PO-1, (ii) supported by clamping at the fibre end of the specimen, called PO-2, and (iii) fibre fragmentation in the single fibre composite, called SFFT. The model is shown to give rather similar but not identical results for the three cases. This facilitates and simplifies the equations for the test cases, which are presented in the same or comparable format.

Two *governing equations* are derived for each test case, one equation relating the fibre load or composite stress to debond length, and the other equation relating the relative displacement/debond length ratio to the debond length. The first equation is very similar for the three cases, and the second equation is identical for the three cases. This latter derivation is a new observation.

These two equations allow two *simple linear plots* and the direct determination of the three interface parameters from the slope and cut-off values of these plots. This is possible (only) when the three experimental parameters are recorded: fibre load, debond length and relative fibre/mtatrix displacement. This is illustrated for the material system of a steel fibre in polyester matrix.

Many *experiments exist* in the literature, which (only) measure the maximum force for pull-out of fibres with different embedded lengths. The mechanical model and the equation for fibre load vs debond length can be used to establish the *true* interfacial shear stress, and (only) a *combination* of interface energy and mismatch strain. This is illustrated for the material system of a steel fibre in epoxy matrix, in test case PO-2, and for the material system of a tungsten wire in copper matrix, in test case PO-1.

It is believed that the *results for the interface parameters* obtained here are correct, but few or no reference values exist to compare and validate the numerical results.

References

[1] Kelly A and Tyson W R 1965 *J. Mech. Phys. Solids* **13** 329
[2] Jones F R 1989 *Interfacial Phenomena in Composite Materials '89* (London: Butterworths)
[3] Verpoest I and Jones F R 1991 *Interfacial Phenomena in Composite Materials* (Oxford: Butterworth-Heinemann)
[4] Hutchinson J W and Jensen H M 1990 *Mechanics of Materials* **9** 139
[5] Sørensen B F and Lilholt H 2016 *Proc. 37th Risø Int. Symp. on Mat. Science,* eds B Madsen et al (Roskilde Denmark : Dept. of Wind Energy, Techn. Univ. of Denmark) p 115 *also* IOP Conf. Series: Materials Science and Engineering **139** 012009
[6] Sørensen B F 2017 *Mechanics of Materials* **104** 38
[7] Budiansky B, Hutchinson J W and Evans A G 1986 *J. Mech. Phys. Solids* **34** 167
[8] Prabhakaran R T D, Gupta M, Lilholt H, Sørensen B F and Mahajan P 2013 *Proc. 34th Risø Int. Symp. on Mat. Science,* eds B Madsen et al (Roskilde Denmark : Dept. of Wind Energy, Techn. Univ. of Denmark) p 341
[9] Piggott M R 1991 *Interfacial Phenomena in Composite Materials*, eds I Verpoest and F R Jones (Oxford: Butterworth-Heinemann) p 3
[10] Meretz S, Nowak H, Hampe A, Hinrichsen G, Schumacher K and Sernow R 1991 *Interfacial Phenomena in Composite Materials*, eds I Verpoest and F R Jones (Oxford: Butterworth-Heinemann) p 73
[11] Auvray M H, Chéneau-Henry P, Leroy F H and Favre J P 1994 *Composites* **25** 776
[12] Scheer R J and Nairn J A 1995 *J. Adhesion* **53** 45

[13] Gorbatkina Yu A and Ivanova-Mumjieva V G 2000 *Mechanics of Composite Materials* **36** 435
[14] Gorbatkina Yu A 1992 *Adhesive Strength of Fiber-Polymer Systems* (New York : Ellis Horwood)
[15] Zhandarov S and Mäder E 2003 *J. Adhesion Sci. and Techn.* **17** 967
[16] Tyson W R 1964 *Fibre Reinforcement of Metals* (Cambridge UK: Thesis)
[17] Kelly A 1973 *Strong Solids* (Oxford: Clarendon Press) second edition p 203